JOURNAL OF MATERIALS SCIENCE 27 (1992) 6053–6061

Phase evolution in Al_2O_3 fibre prepared from an oxychloride precursor

P. G. LUCUTA, J. D. HALLIDAY
AECL Research–Chalk River Laboratories, Chalk River, Ontario, Canada KOJ 1J0
B. CHRISTIAN*
Fiberglas Canada Inc., Technical Research Centre, Pt. Edward, Ontario, Canada N7T 7X4

The formation of polycrystalline α-alumina during the heat treatment of aluminium oxychloride fibres occurs via transitions through various intermediate crystalline alumina phases. The different phases show a strict pseudomorphism, i.e. the external shape of the crystal is retained and there is an orientational relationship between the crystal axes, before and after the phase transition. Consequently, the phase sequences and microstructure are interdependent and controlled by the heat-treatment conditions, which determine the final properties of the fibres. The effects of water content in the fibre formulation, and sintering temperature and heating rate on the phase development from amorphous oxychloride to crystalline α-alumina fibres, were investigated. The transition path for the phase evolution during heat treatment to 1200 °C (when the formation of α-alumina is completed) was established and correlated with fibre microstructure. In fibres with higher water content, the transition temperature for γ- and δ-alumina phase formation was higher. Only for a very high heating rate was θ-alumina observed as an intermediate phase during phase evolution. The axial porosity appeared to be eliminated more rapidly in the fibres at temperatures below 1200 °C. Consequently, residual porosity, comprising closed pores, in the final stage of sintering, was mainly observed radially oriented toward, and on, the fibre surface. A high diametral shrinkage was measured and plotted as a function of the sintering temperatures used for fibre heat-treatment.

1. Introduction

Ceramic fibres, in particular alumina fibres, are of growing interest and importance for a variety of applications, from high-temperature insulation to metal and polymer reinforcement [1–10]. The fibre properties are determined by the microstructure formed during the transition from the amorphous to polycrystalline α-alumina phase in the sintering process [3–10]. It is well known that α-alumina formation occurs in monolithic ceramics through various transitional aluminium oxide phases. Boehmite transforms into α-alumina through intermediate polycrystalline γ-, δ- and θ-alumina phases as the temperature increases [11, 12]. Nevertheless, there are persistent problems in α-alumina synthesis involving the transformation path and microstructural evolution. The last sequence of the transformation results in gross microstructural changes. Chemically controlled nucleation can tailor the microstructure by diminishing the grain growth [11–13].

The microstructure of alumina fibres differs considerably from traditional monolithic alumina ceramics. In particular, the crystallite and pore size are on a much finer scale. This requires close control and adjustment of the sintering process. Most studies on alumina fibre synthesis, microstructure and properties [1–10] used fibres containing 2 to 20 wt % silica as a second component to control the microstructure [3–7], although pure α-alumina fibres are currently produced [1, 2]. α-alumina fibres have also been prepared by a unidirectional freezing route and the phase evolution has been determined [8, 9]. This paper describes the phase evolution from amorphous aluminium oxychloride to pure polycrystalline α-alumina in fibres, during heat treatments at temperatures from 200 to 1200 °C, using a heating rate of 600 °C h^{-1}. Very high heating rates (70 to 3000 °C s^{-1}) and significantly shorter soak times were also investigated. A transformation path similar to the transition from boehmite to α-alumina, with the various transitional phases coexisting, was identified. Some typical aspects related to fibre densification are also outlined.

2. Experimental procedure

An aluminium oxychloride solution with a viscosity in the range 2000 to 4000 cP (mPa s), with polyethylene oxide and polyvinylpyrrolidone (about 5 wt %) included as fibreizing agents, was used to produce fibres. These were spun and blown through a tubular furnace

---

* *Present address*: Northern Telecom Canada Ltd, Belleville, Ontario, Canada K8N 5B7.

0022–2461 © *1992 Chapman & Hall*

heated at 500 °C that raised the estimated fibre temperature to 150–200 °C. Batches of fibre were prepared from solutions with differing solid to water ratios (s/w): one with $s/w = 13/7$, defined as low water-content fibres (LWC), and a second with $s/w = 5/6$ (high-water content batch of fibres (HWC)). Both formulations produced continuous "green" fibres with a nominal diameter of 24 µm. Samples of "green" fibres (about 5 g each) were then heat-treated in air at various temperatures ranging from 200 to 1200 °C, using a heating rate of $600\,°\mathrm{C\,h^{-1}}$ and 1 h soak time, and investigated for crystalline phases and microstructure.

A third batch of fibres from the LWC formulation was dried during preparation by increasing the fibre apparatus furnace temperature to 900 °C, so these "dry" fibres attained a temperature of about 350–400 °C. The dry LWC fibres were used to investigate high heating rates (in the calculated range of 70 to $3000\,°\mathrm{C\,s^{-1}}$ and corresponding soak times of 15 to 0.25 s), by passing a bundle with a constant speed through a tubular furnace preheated at 1600 °C. The various speeds used to pull the specimen, in the range of 1.5 to $80\,\mathrm{cm\,s^{-1}}$, provided the different heating rates and times through the hot zone (the region with a temperature higher than the transition temperature to α-alumina).

The fibres, fired at various temperatures, were rapidly cooled and the various phases were determined on powder specimens by X-ray diffraction (XRD). Differential thermal analysis (DTA) was used on the green fibres over a temperature range from 25 to 1400 °C, with a $10\,°\mathrm{C\,min^{-1}}$ heating rate. The weight loss between room temperature and 900 °C was recorded by thermogravimetric analysis (TGA). Microstructural features of the fibres were revealed by scanning electron microscopy (SEM) of the fibre surfaces and fractured cross-sections.

3. Results

The phase development from amorphous aluminium oxychloride to highly crystalline α-alumina fibres takes place through several transitional phases. The diffraction patterns of the HWC and LWC fibres, heat-treated at various temperatures between 200 and 1200 °C, using a heating rate of $600\,°\mathrm{C\,h^{-1}}$, are shown in Fig. 1, and demonstrate the different alumina phases formed. The DTA plot from the HWC fibres showed a strong endothermic reaction in the 100 to 350 °C temperature range, followed by an exothermic peak at 400 °C and two more small exothermic peaks at 920 and 1140 °C (Fig. 2). For the LWC fibres, the DTA showed similar features: an even stronger endothermic peak between 100 and 400 °C and three exothermic peaks, with the second peak displaced toward a lower temperature (790 °C). Total weight losses of 53 and 50 w % were determined for the HWC and LWC fibres, respectively (Fig. 3). The small difference shows that the HWC "green" fibres lost more water during fabrication. The weight loss rises rapidly in the 100 to 500 °C range and increases slowly up to 1000 °C.

The green fibres displayed a typical amorphous diffraction pattern (Fig. 1) with two very broad peaks. The fibre surface was smooth and featureless and the average fibre diameter was estimated to be 23 µm, by a linear interception method, from ten different SEMs (Fig. 4). On heating the fibres to 350–400 °C, most of the water and chlorine was lost and the aluminium oxychloride decomposed into amorphous aluminium oxide hydroxide. This stage corresponds to the endothermic peak in the DTA curve (Fig. 2) and explains the high weight loss observed in this temperature range (Fig. 3). The stronger endothermic peak intensity recorded for the LWC fibres suggests a higher energy of the reaction due to the greater oxychloride content. A larger oxychloride content means more HCl had to be removed, a fact confirmed by the measurements of the Cl content in the fibres.*

γ-alumina crystallized at 400 and 700 °C for the LWC and HWC fibres, respectively (Fig. 1). The broad peaks of the diffraction pattern are explained by the very fine crystallites nucleated from the amorphous fibres. A few other weak reflections (arrows in Fig. 1) belong to some crystallized aluminium oxide hydroxide formed in the LWC fibres at 400 °C. These reflections disappeared as the firing temperature was raised to 600 °C. The nucleation of $\gamma\text{-Al}_2\text{O}_3$ occurred at a higher temperature (700 °C) in the HWC fibres than in the LWC fibres (400 °C). The exothermic peak around 400–450 °C in the DTA does not involve γ-alumina formation. The DTA run for the fibreizing agent and the black colour of the fibres heat-treated at 400 and 500 °C were evidence that the exothermic reaction is due to the pyrolysis of the fibreizing agent. The formation of $\gamma\text{-Al}_2\text{O}_3$ does not change the fibre microstructure drastically. The fibres retain the smooth surfaces of the amorphous green stage. Tiny, submicrometre crystallites constitute the microstructure, as shown in the SEM of a fibre fractured surface (Fig. 5a).

With increased firing temperature, a mixture of γ- and δ-aluminas coexists at 800 and 900 °C for the LWC and HWC fibres, respectively (Fig. 1). The presence of the δ-phase is revealed by its distinct reflections. The transition from γ- to δ-alumina involves an exothermic reaction marked by the exothermic peaks at 790 and 920 °C in the DTA curve for the LCW and HCW fibres, respectively. The diameter of the LWC fibres heat-treated at 800 °C ranges from 17 to 21 µm with an average diameter of 18 µm, representing a diametral shrinkage of 22% (Fig. 4). Fracture surfaces show tiny crystallites in a relatively dense inner core (about 10 µm wide) and slightly larger crystallites in an outer shell (Fig. 5b). Small pores (< 0.2 µm) are also observed in the outer shell. The porosity increases along the radius toward the fibre surface. A thin, compact layer shields the outer shell. The two regions reflect the presence of the two alumina phases found by XRD: γ-alumina crystallites

---

* The amount of Cl measured from the LWC fibres heat-treated at 100 °C was 15.2 wt % and decreased to 0.5 wt % at 400 °C, compared to 9.9 wt % at 100 °C and 0.3 wt % at 400 °C determined for the HWC fibres; at 800 °C, about 0.03 wt % Cl was found in both fibre batches.

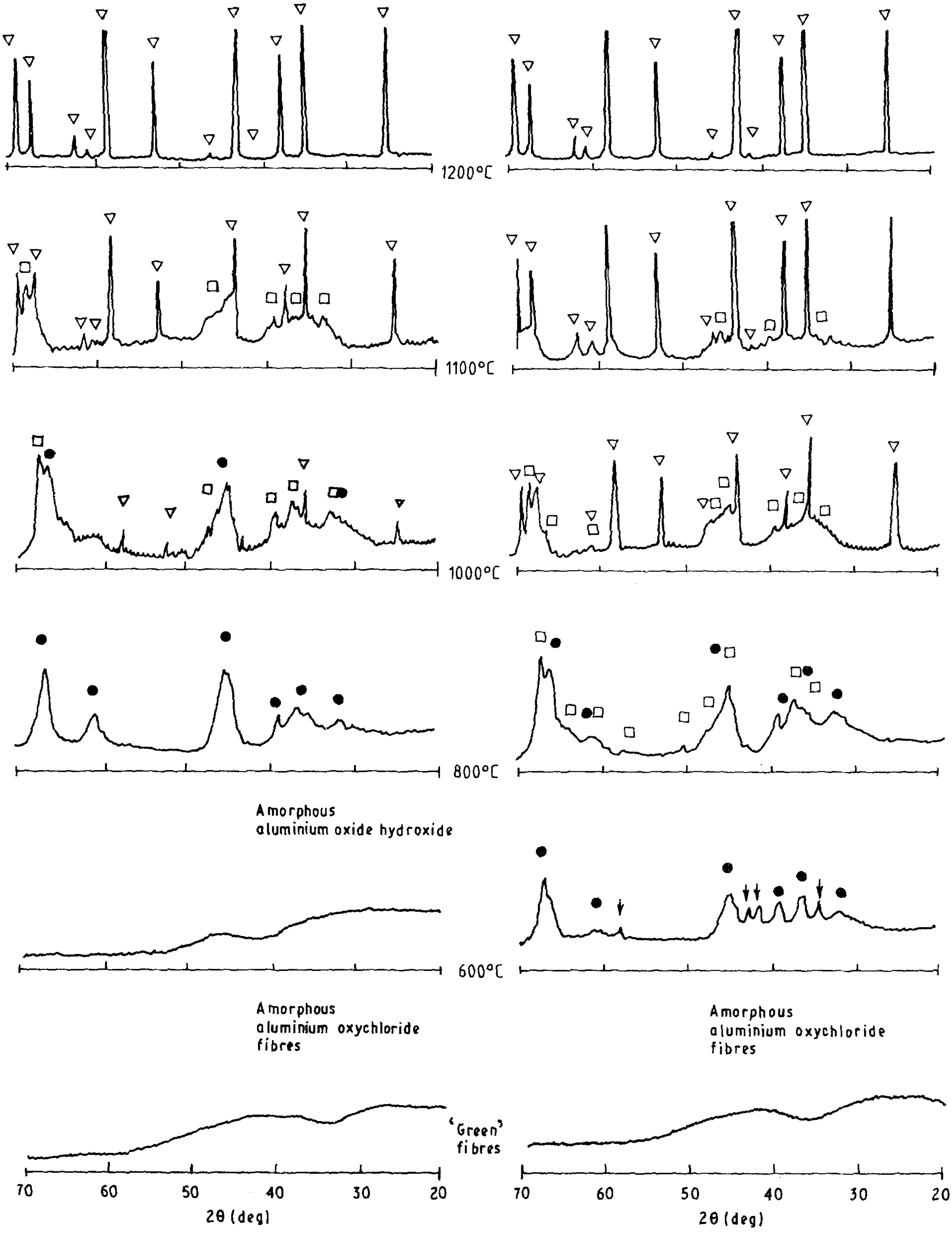

Figure 1 Phase evolution in alumina fibres with low and high water content as function of firing temperature. The X-ray diffraction patterns were recorded at room temperature. (▽) α-, (□) δ-, (●) γ-alumina; (↓) aluminium oxide hydroxide.

constitute the inner core with δ-alumina formed in the outer shell.

At higher firing temperatures, 900 °C for the LWC fibres and 1000 °C for the HWC fibres, δ-alumina is the major phase along with some remanent γ-phase, as well as newly formed α-alumina. The reflections of δ- and γ-phase are broad compared with those of the well-crystallized α-phase. The occurrence of the α-phase and the presence of γ-alumina at these temperatures suggest a direct transformation of γ-into α-alumina, which is known to take place at lower temperatures than the transition from δ- to α-alumina [4]. α-alumina (about 38 vol % for LWC fibres and 7 vol % for HWC fibres, estimated from the intensity of the XRD reflections) is formed from γ-alumina at 1000 °C. The weight loss of 6% recorded for temperatures in the range of 600 to 1000 °C (Fig. 3) can be explained by the loss of surface-bond groups in the fibre structure. The LWC fibre diameters, after heat-treatment at 900 °C, range from 14 to 20 μm, with an

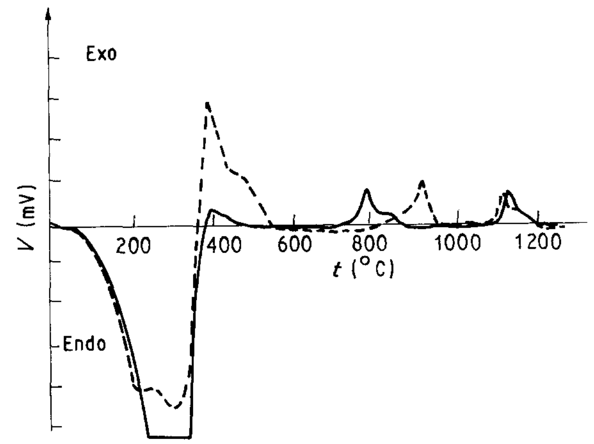

Figure 2 Differential thermal analysis of alumina fibres with (——) low and (- - -) high water content.

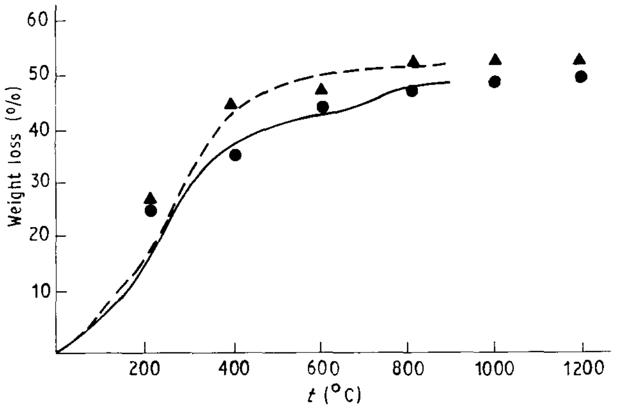

Figure 3 Weight loss of alumina fibres versus firing temperature; the curve was recorded by TGA and the weights denoted by symbols were measured during heat-treatment tests for XRD analysis. LWC fibres: (——) TGA, (●) weight. HWC fibres: (- - -) TGA, (▲) weight.

average value of 16.5 μm, which corresponds to a shrinkage of 28% (Fig. 4). The fracture surface shows a homogeneous microstructure with small pores radially oriented in the fibre cross-section.

The amount of α-alumina increases as the temperature increases. At 1100 °C, α-alumina is the main phase, along with a small amount of δ-alumina still present in both fibre batches. No evidence of θ-alumina was found in the XRD patterns. The transformation of δ- into α-alumina is defined by the exothermic peak just above 1100 °C in the DTA curve of both batches (Fig. 2). The surface of the HWC fibres heat-treated at 1100 °C presents numerous submicrometre pores. The fracture surface shows a dense inner core formed by small crystallites and an outer region with a radial alignment of larger crystallites (Fig. 6c). The coexistence of the α- and δ-aluminas detected by XRD and the microstructure suggest that the core region consists of δ-alumina crystallites and, in the outer shell, α-alumina grains formed with radial orientation. The radial pore distribution in the cross-section, and the presence of surface porosity, hint toward radial removal of the pores. Radially oriented pores were previously observed in Al_2O_3–SiO_2 fibres [3]. The fibre densification starts practically only at this temperature, when the phase development is almost completed.

At a sintering temperature of 1200 °C, highly crystalline α-alumina fibres were obtained (Fig. 1). The complete formation of α-phase at this temperature is reflected in the fibre microstructure formed by small grains of α-alumina elongated along the fibre radius (Fig. 5d). A small remnant internal porosity is still present. However, most of the pores migrated toward the fibre surface, increasing the surface porosity. The average fibre diameter was estimated as 13.5 μm (diametral shrinkage of 41%) (Fig. 4).

A rapid sintering cycle consisting of high heating rates and short soak times is an attractive approach for a preparation–sintering on-line production of the alumina fibres. Experimental results using various speeds through a furnace preheated to 1600 °C showed that the transition from amorphous to polycrystalline γ-alumina was attained for the highest speed (0.25 s through the hot zone). γ-alumina was identified by broad XRD peaks (Fig. 6) and about 75% crystallinity was estimated. In spite of the high heating rate, no major disruptions or damage were observed in the fibre microstructure (Fig. 7). As the speed decreased (lower heating rate and longer time through the hot zone), transitional alumina phases corresponding to higher temperature formed in the fibres (Fig. 6). Although similar transitional alumina phases were identified for the high heating rates and a regular heating rate of 600 °C h^{-1}, from a kinetics point of view the phase transformation processes may be different. θ-alumina, which has not been found in the fibres heat-treated at various temperatures using the 600 °C h^{-1} heating rate, was also identified for a heating rate of 400 °C s^{-1}, along with δ- and α-alumina (Fig. 6). For the lowest speed of 1.5 cm s^{-1} (heating rate 70 °C s^{-1}; 15 s through the hot zone) mainly α-alumina formed, but the transformation was not completed (some remnant δ-alumina was present). The fast firing cycles yielded transformation into different transitional alumina phases without major disruptions in the fibre microstructure.

4. Discussion

The formula $Al_2(OH)_5Cl$ for aluminium oxychloride defines only the degree of hydrolysis and does not correspond to a stoichiometric compound; rather, it refers to a complex mixture of amorphous species, which is the precursor for alumina fibres in many patented preparation routes [10]. However, the phase development from amorphous oxychloride to polycrystalline α-alumina fibres has not been investigated in these previous studies.

The experimental results in this investigation show that phase evolution in fibres prepared from aluminium oxychloride involves several transitional stages before highly crystalline α-alumina is formed:

Aluminium oxychloride (amorphous) → Aluminium oxide hydroxide (amorphous) → $\gamma\text{-}Al_2O_3$ → $\delta\text{-}Al_2O_3$ → $(\theta\text{-}Al_2O_3)$ (at very high heating rates) → $\alpha\text{-}Al_2O_3$

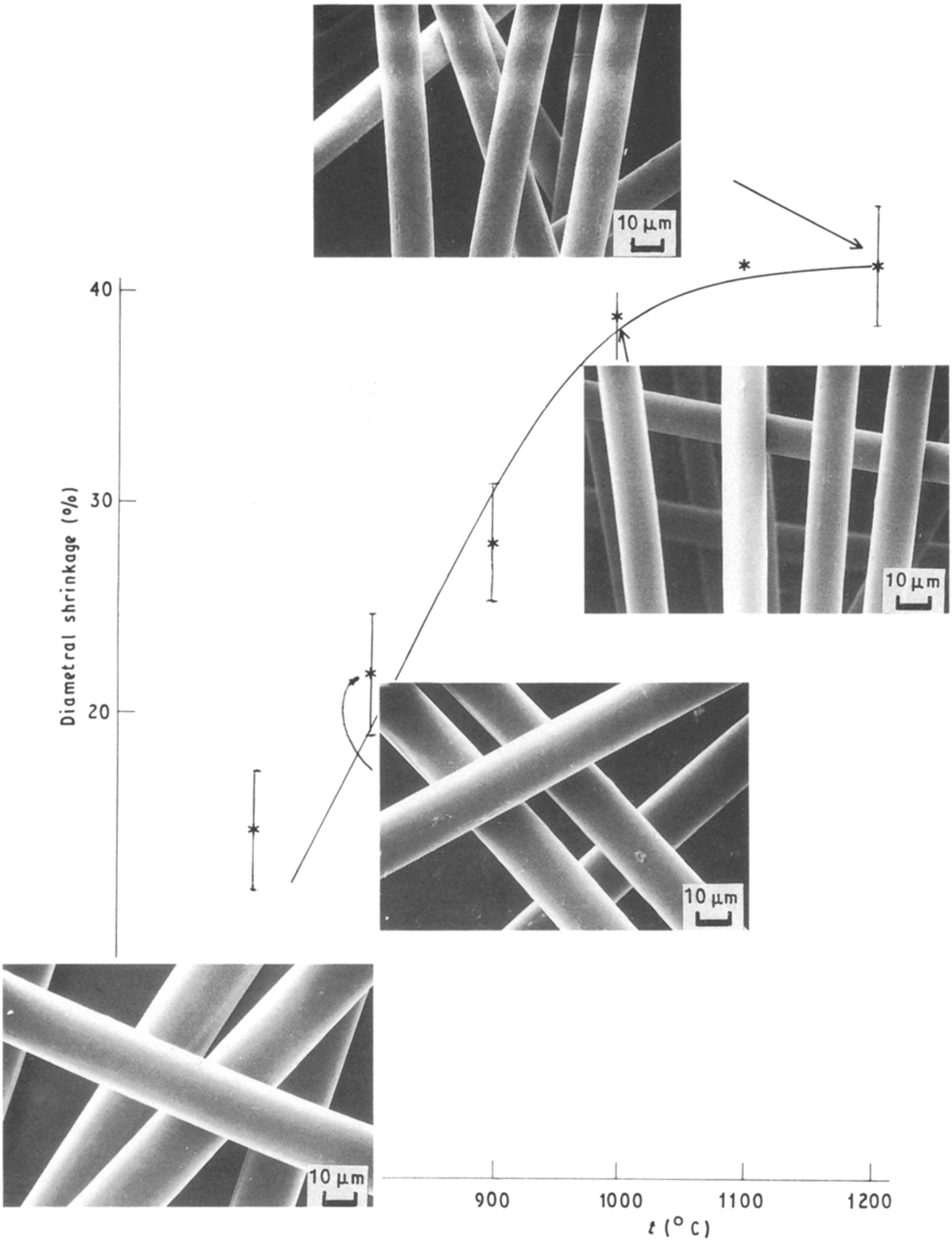

Figure 4 Diametral shrinkage for various firing temperature and corresponding scanning electron micrographs of the heat-treated fibres.

The water content in the fibre formulation did not change the transformation path, but significantly shifted the transitional alumina phases toward higher transformation temperatures for the HWC fibres (Fig. 8). This path is similar to that reported for boehmite transformation [3], except that θ-alumina was identified in the fibres only for one high heating rate. In the first stage, the aluminium oxychloride decomposes into amorphous aluminium oxide hydroxide by a strong endothermic reaction. In previous work [8], aluminium oxychloride was decomposed into aluminium oxide hydroxide, which was then incorporated in a sol used to form fibres by unidirectional freezing. Fibres were found to form only from sols that contained mostly amorphous aluminium oxide hydroxide particles. This result is consistent

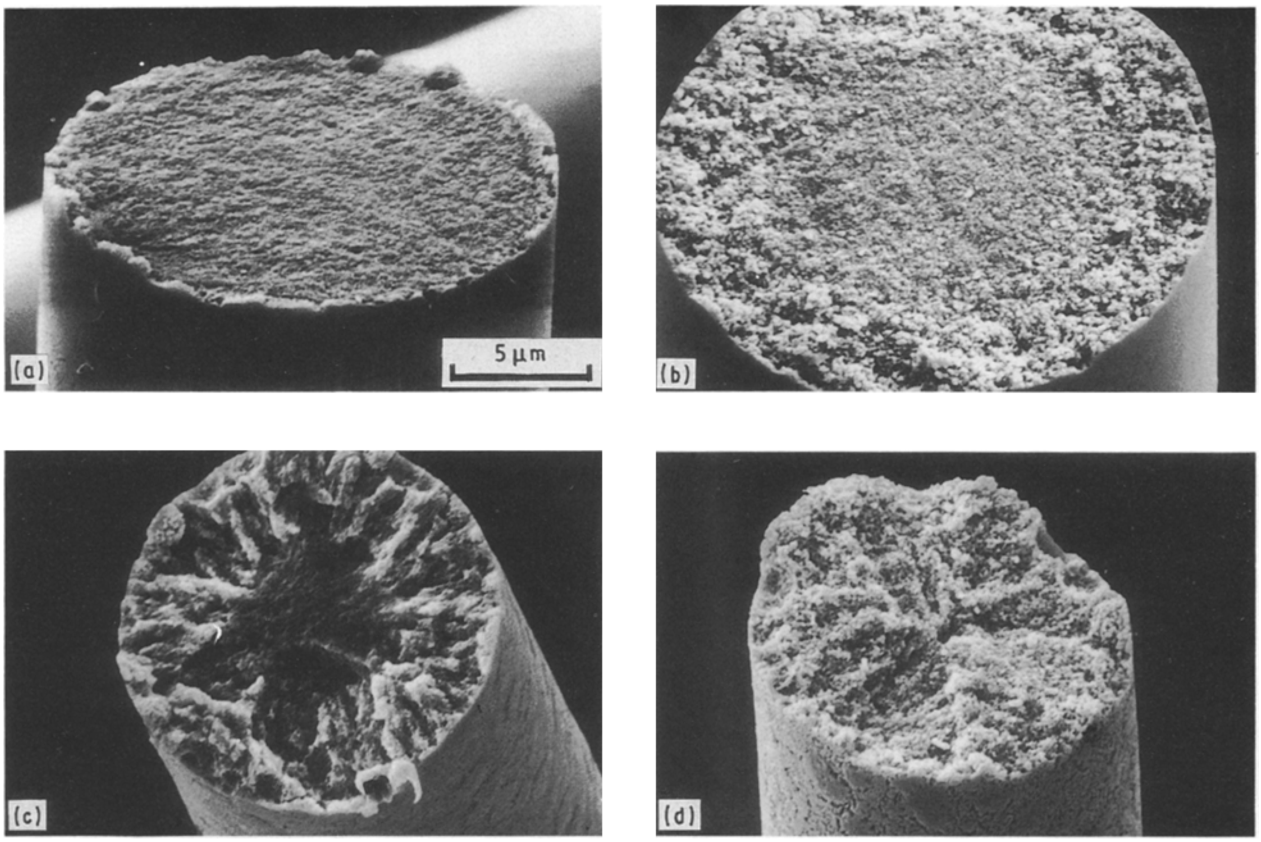

Figure 5 Secondary electron images of fibre cross-sections showing the fibre microstructure for the various firing temperatures (HWC fibre batch): (a) 700 °C, (b) 900 °C, (c) 1100 °C, (d) 1200 °C.

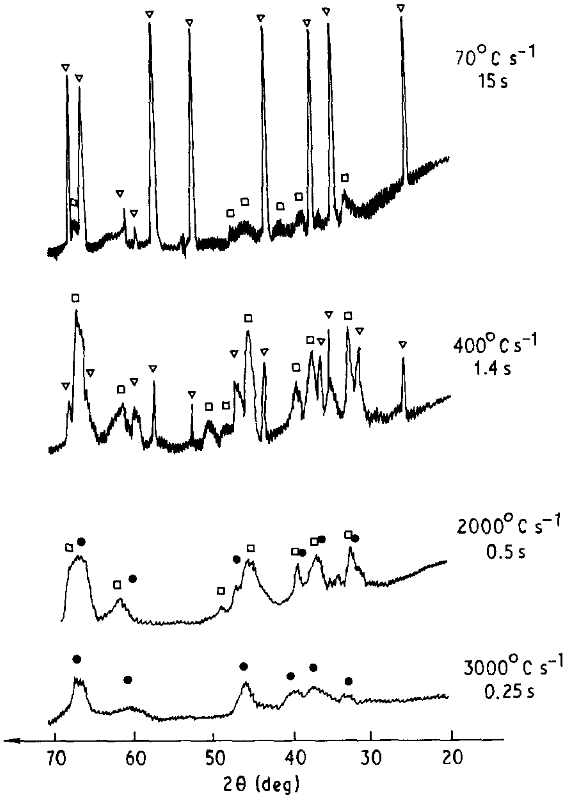

Figure 6 Phase evolution in alumina fibres fired at high heating rates. The diffraction patterns were recorded at room temperature. (▽) α-, (□) δ-, (●) γ-alumina.

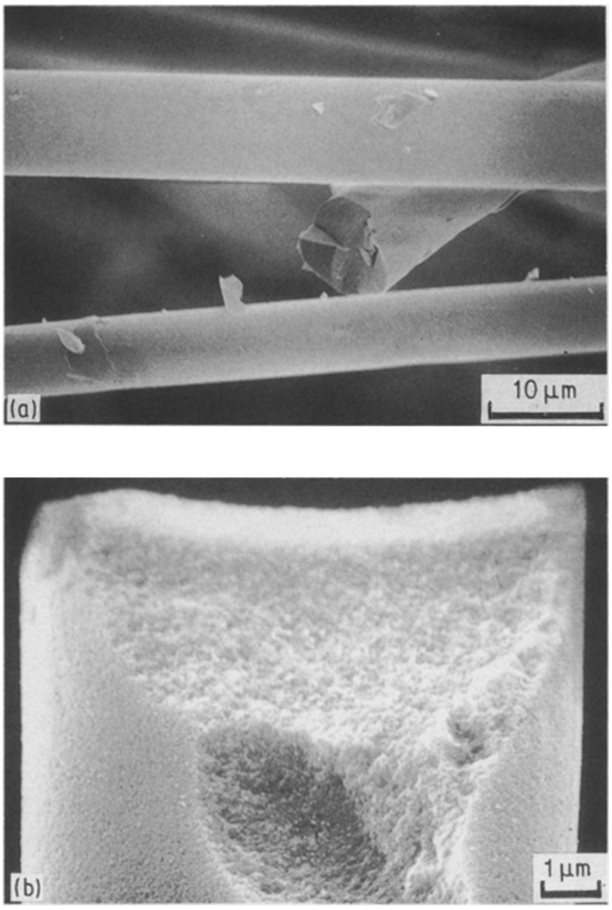

Figure 7 (a) Fibre surface and (b) microstructure after heat-treatment using a heating rate of 3000 °C s^{-1} (0.25 s through the hot zone).

with the decomposition of the oxychloride into amorphous aluminium oxide hydroxide observed in the first stage of the phase evolution in our fibres.

Crystalline γ-alumina formed from amorphous

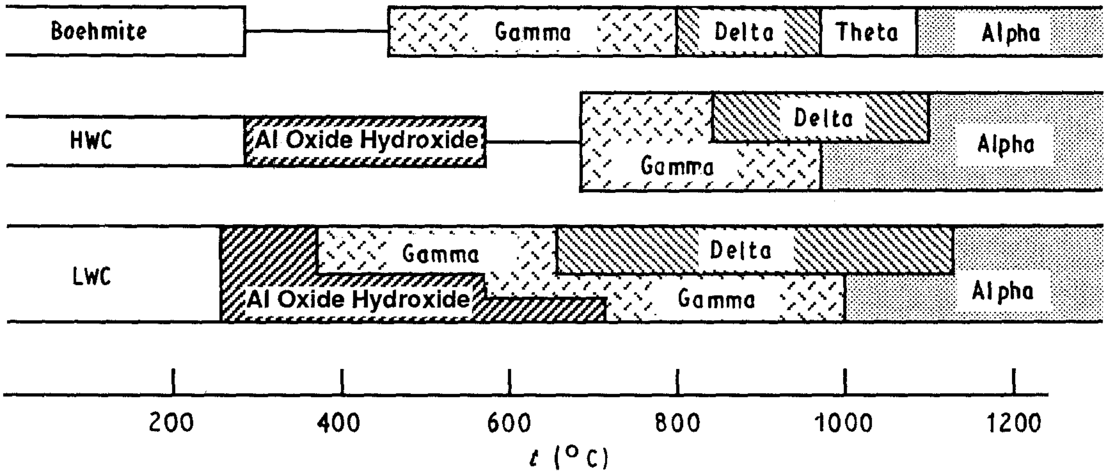

Figure 8 Phase evolution identified in alumina fibres with low and high water content, prepared from aluminium oxychloride, compared with the transformation from boehmite to α-alumina.

aluminium oxide hydroxide at a lower temperature (400 °C) in the LWC fibres, and at a higher temperature (700 °C) in the HWC fibres, compared with the 500 °C reported for the boehmite transformation [3]. γ-alumina was found to exist through an extended temperature range in both batches of alumina fibres. The formation of the γ-alumina phase at a lower temperature in the LWC than in the HWC fibres might be related to differences in the aluminium oxide–hydroxide species due to the water content, that lead to an earlier nucleation for the LWC fibres. In the alumina fibres prepared by unidirectional freezing [8, 9], η-alumina has been reported to form from aluminium oxide hydroxide. In fact, the X-ray reflections of the γ- and η-alumina are overlapped but the intensities are different. In fibres, the intensities can be altered by preferential orientation, which is eliminated for powder specimens.

The transition from γ- to δ-alumina involves an exothermic reaction at 790 and 920 °C for the LWC and HWC fibres, respectively. These DTA results are supported by the XRD results that identified δ-alumina at 800 and 900 °C, respectively. The temperature span of the δ-alumina phase is shifted towards lower temperatures for the LWC fibres. The transition takes place gradually over a temperature range of about 300 °C for the LWC (700 to 1000 °C) and 100 °C for the HWC fibres (900 to 1000 °C), respectively. The fibre microstructure reflects the existence of the two phases in the SEM micrographs of fibre cross-sections.

The exothermic δ → α transition occurred at the same temperature of 1125 °C in both LWC and HWC fibre batches. However, α-alumina was already detected in the LWC and HWC XRD patterns at 900 and 1000 °C due to the direct transformation of γ- into α-alumina that takes place in alumina fibres at lower temperature. Thus, α-alumina is formed in fibres by the direct transformation of γ- into α-alumina in the 900 to 1100 °C temperature range and by the transition of δ into α at temperatures above 1100 °C. The transition temperature from δ to α, defined by the exothermic peak in the DTA, is in good agreement with the previously reported data [3, 4]. θ-alumina, found as a transitional phase for high heating rates, might exist as well in a narrow temperature range for the low heating rate of 600 °C h^{-1}.

The XRD data show a close pseudomorphism for the various identified transitional phases. The external shape of the crystal is retained and there is an orientational relationship between the crystal axes, before and after the phase transition. The differences in the XRD patterns of transitional alumina phases (Fig. 2) are due to the redistribution of the Al ions in the interstices of the oxygen lattice. The cubic close-packed oxygen structure is preserved through the various transitions [3]. This can explain the relatively strong fibres obtained after each heat-treatment stage. Transmission electron microscopy (TEM) and selected-area electron diffraction (SAED) on the fibres heat-treated at 1100 °C brought additional evidence of the pseudomorphism. The SAED from a fibre chip (Fig. 9a) showed the coexistence of the newly nucleated α- and remnant δ-alumina crystallites with related orientation of the crystal axis (Fig. 9b).

Consequently, the phase sequences and the microstructure are interdependent. The fibre formulation and the heat-treatment conditions affect the phase development and are related to the microstructure. A critical step is the formation of α-alumina at lower temperatures directly from γ-alumina. This can cause excessive grain growth in some regions and create disruptions in the fibre microstructure.

The diametral shrinkage of the fibres, summarized as a function of the temperature, is also plotted in Fig. 4. The error bars were estimated from the statistical error of the fibre diameter measurements. The data show a higher rate of shrinkage before the α-alumina is formed, explained by the volume changes involved in the phase transition from γ- to δ/α-aluminas. A similar high rate of linear shrinkage was previously reported in alumina–silica fibres for the various transition phases heated up to 1400 °C [7]. Volumetric shrinkage of alumina fibres was previously determined from density and porosity data [5]. Compared with the diametral shrinkage, the volumetric shrinkage is lower. The mismatch between the two sets

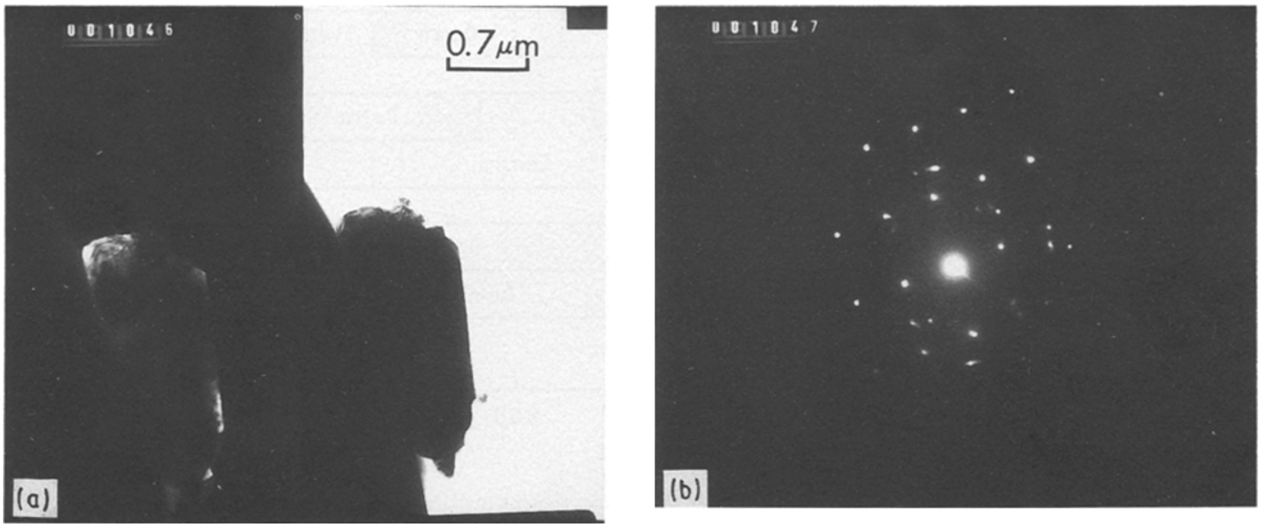

Figure 9 (a) TEM micrograph from alumina fibre chip sintered at 1100 °C; (b) associated SAED pattern with contribution from two different crystallites corresponding to α- and δ-phases with related crystal axes.

of data can be attributed to a non-isotropic shrinkage and, consequently, a much lower axial shrinkage should take place in the fibres.

The fibre surfaces are smooth, even at temperatures above 1100 °C where densification effects were observed. The axial porosity appears to be eliminated at 1200 °C. The remnant porosity is radially distributed and the pores migrate to the fibre surface (Fig. 5c and d). Sintering at higher temperature reduces the porosity, but extensive radial grain growth occurs. The phase development from amorphous to polycrystalline alumina can be achieved in fibres by a fast firing process.

5. Conclusions

In summary, this investigation pointed out some general features of the phase evolution in alumina fibres prepared from an oxychloride precursor, as well as some aspects related to fibre formulation and firing conditions. The phase sequences and microstructure are interdependent and controlled by the heat-treatment conditions, which determine the final fibre properties. In particular, for a heating rate of 600 °C h^{-1}:

1. The transformation path for alumina fibres prepared from an oxychloride precursor is similar to the phase evolution from boehmite to α-alumina.
2. The formulation and/or firing conditions affect the phase evolution by shifting the temperature range of the transitional alumina phases.
3. The decomposition of oxychloride into aluminium oxide hydroxides takes place below 400 °C by a strong endothermic reaction and the transitions from γ- to δ-alumina, and δ- to α-alumina, are marked by exothermic reaction.
4. A direct transition from γ- to α-alumina was observed to take place in fibres around 1000 °C before the usual transformation of δ- into α-alumina above 1100 °C.
5. Highly crystalline, monophase, α-alumina fibres are obtained at temperatures of 1200 °C and above, with a homogeneous microstructure and small remnant porosity.
6. The different transitional phases show a strict pseudomorphism, so the phase sequences and microstructure are interdependent and controlled by the heat-treatment conditions.
7. The axial porosity appears to be eliminated more rapidly and, consequently, the residual porosity consists of small closed pores, mainly radially oriented toward/on the fibre surface at 1200 °C.

Polycrystalline fibres without any major disruptions in the microstructure were attained with a fast firing process.

Acknowledgements

The authors wish to thank D. Lethbridge for fibre preparation and L. E. Bahen and D. S. Hartwig for SEM investigations, as well as Dr P. Hayward for critical review of the manuscript. The helpful discussions with Dr K. Linger and Dr N. Cameron from Fiberglas Canada, and B. J. F. Palmer (presently at Westaim Technologies, Fort Saskatchewan, Alberta) and Dr J. D. Sullivan from AECL Research and their involvement in project management, is also acknowledged.

References

1. A. K. DHINGRA, *Phil. Trans. R. Soc.* **A294** (1980) 411.
2. *Idem., Chemtech.* No. 10 (1981) 600.
3. J. D. BIRCHALL, J. A. A. BRADBURY and J. DINWOODIE, in "Handbook of Composites", Vol. 1, edited by W. Watt and B. V. Perov (Elsevier Science, London, 1985) p. 115.
4. J. D. BIRCHALL, *Trans. J. Br. Ceram. Soc.* **82** (1983) 143.
5. M. H. STACEY, in "Science of Ceramics", Vol. 14, edited by D. Taylor (Institute of Ceramics, Stoke-on-Trest, UK, 1988) p. 291.
6. *Idem., Trans. J. Br. Ceram. Soc.* **87** (1988) 168.

7. E. RASTETTER and W. R. SYMES, *Interceram.* No. 3 (1982) 215.
8. T. MAKI and S. SAKKA, *J. Mater. Sci. Lett.* **5** (1986) 28.
9. T. MAKI, T. KOKUBO and S. SAKKA, *Bull. Inst. Chem. Res. Kyoto Univ.* **64**(4) (1986) 292.
10. Patents on alumina fibres: USA 3 322 865 (1964), 3 503 765 (1966), 3 579 361 (1969); FRG 1 918 754 (1969), 2 054 573 (1970); UK 1 360 197 (1974), 1 360 199 (1974), 1 360 200 (1974), 1 402 544 (1975), 1 425 934 (1976).
11. G. L. MESSING, R. A. SHELLEMAN and J. L. McARDLE, in "Science of Ceramics", Vol. 14, edited by D. Taylor (Institute of Ceramics, Stoke-on-Trest, UK, 1986) p. 101.
12. R. A. SHELLEMAN, G. L. MESSING and M. KUMAGAI, *J. Non-Cryst. Solids* **82** (1986) 277.
13. J. L. McARDLE and G. L. MESSING, *Adv. Ceram. Mater.* **3** (1988) 387.
14. M. DAUZAT, M. PIJOLAT and M. SOUSTELLE, in "Science of Ceramics", Vol. 14, edited by D. Taylor (Institute of Ceramics, Stoke-on-Trest, UK, 1986) p. 491.

Received 2 July 1991
and accepted 7 February 1992